ID: 598

Advanced Characterization of Cretaceous Carbonate Reservoirs in South Iraq Using Nuclear Magnetic Resonance Logs and Electrical Borehole Images

Wassem Alward[1], Mohammed Al-Jubouri[1], Xu Xiaori[2], Ling Zongfa[2], Jin Rongrong[3], Cui Yi[2]

(1) SLB, Iraq
(2) China National Oil &Gas Exploration & Development Company, Iraq
(3) Research and Institute of Petroleum Exploration and Development, PetroChina, China

ABSTRACT

The cretaceous carbonate reservoirs in South Iraq are long known for exhibiting highly varying properties within small sections of the reservoir, making it difficult to simulate and history-match. The heterogeneity of these reservoirs still has a high uncertainty in southern Iraq where oil production and water-cut continue to prove to be challenging to model, requiring continuing refinement of static models. A focused approach involving a detailed understanding of the fluids saturation, pore-size distribution, permeability, rock texture, reservoir rock type, and natural fracture systems at different scales is needed. With the absence of core data, different log measurements are needed to build a realistic model of the petrophysical properties, the conventional resistivity and porosity measurements are often not sufficient to resolve changes in pore size and texture, so additional measurements are required; particularly borehole images and nuclear magnetic resonance that can extract information on different textural elements and porosity types. Electrical borehole images and NMR logs were acquired in multiple wells in a cretaceous carbonate reservoir in South Iraq. Borehole images were integrated with other petrophysical data to classify different types of pore space: connected to vugs, isolated vugs, connected to fractures, aligned at bed boundaries, or within the rock matrix. The contribution of these different pore types to the total porosity of the formation was quantified in addition to the geometric information of different types of heterogeneities. NMR log data was analyzed using gaussian decomposition technique to locate and extract the volumes of three separate pore body modes. The resultant outputs of macro, meso, and microporosity best reconstruct the input NMR spectrum and provide the permeability heterogeneity corresponding to the different pore sizes. This info, further integrated with borehole image analysis results can characterize the carbonate in such details that are needed to quantify high-resolution textural details, capillary pressure, and pore-network geometry to realistically model such reservoirs that honor and predict the production within optimal tolerance. This study presents the impact of facies heterogeneity on the evaluation of the Cretaceous carbonate reservoirs in the South of Iraq and presents a comprehensive workflow to evaluate and characterize carbonate porosity and permeability systems in non-cored wells.

EXTENDED ABSTRACT

INTRODUCTION

The cretaceous reservoirs in the South of Iraq are proven prolific reservoirs and have been producing for decades, many of which are now undergoing secondary recovery. M reservoir in the study area is 250-300m of carbonates mainly composed of reef-shoal deposits and associated with lagoon carbonates. These carbonates exhibit extreme variability in reservoir properties, and relative sea-level changes in combination with local diagenetic processes such as dissolution, karstification, and cementation through time have controlled the lateral and vertical distribution of these facies and significantly modified pore space and permeability. Due to this heterogeneity, the production profile rarely matches the simulation model, and a lot of manual adjustments are often needed to further refine the static model. The principal challenge for an accurate evaluation of this reservoir is accounting for reservoir heterogeneity on different scales: grains, pores, and textures. Standard log measurements did not fully capture this heterogeneity, leading to inaccurate reservoir predictions and poor rock typing that did not reflect performance variability observed on production and other dynamic data. To achieve a better understanding of how reservoir heterogeneity affects performance and which zones contribute to flow in this reservoir, developing a reliable log-based interpretation methodology is essential, especially when core data are unavailable.

METHODOLOGY

The methodology presented in this paper integrates a comprehensive suite of petrophysical logging measurements for the quantitative determination of the producibility and textural analysis of the M reservoir with a focus on characterization and size partitioning of the pore system using texture-sensitive log measurements: nuclear magnetic resonance (NMR) and high-resolution borehole images. The partitioning analysis is then used in sequential steps to determine carbonate rock types, permeability, and fluid saturation (Figure 1).

Lithology and porosity are derived from a combination of measurements (spectroscopy, density, PEF, neutron, GR), these logs are used in an optimized simultaneous equation solver to derive the volume of each formation component (minerals and fluids), then, it calculates the formation properties from the derived volumes. Spectroscopy measurements are particularly important for carbonate mineralogy as it measures elemental concentrations including magnesium and sulfur which can be respectively used to accurately discriminate dolomite from limestone and estimate anhydrite volume.

The total porosity is partitioned into different pore types based on pore-throat size, jointly using NMR T2 relaxation time and image logs. First, the heterogeneity-based image porosity partitioning method is applied to extract the volume of different types of pore space: connected vugs, isolated vugs, pores connected to fractures, aligned at bed boundaries, and within the rock matrix. Image processing techniques are applied to extract the different textural heterogeneities (resistive, conductive) which are then combined with interpreted dips (bedding, fractures, stylolites, etc) and other geometrical parameters (such as connectedness) to produce a classified heterogeneity image. The resistivity image is converted into a porosity image using a modified Archie equation. The porosity image is combined with the classified heterogeneity image generated from the previous step to classify the porosity values in the porosity image (Figure 2). (Yamada, 2013) and (Noufal, 2018) presented a detailed account of this method, validated by core results and dynamic data. In the M reservoir, vugs represent the most dominant form of secondary porosity, therefore, accurate estimation for this type of pore space is essential for productivity analysis and for which borehole images are particularly suitable.

The vuggy porosity from the image-log porosity partitioning method is used to augment the porosity partitioning from NMR T2 relaxation time and to address the measurement distortion induced by oil saturation effects, insufficient polarization, diffusion as well as truncation of T2 distribution at large relaxation time. The NMR T2 relaxation time in the M reservoir exhibit multimodal pore-body distributions which have been verified with core samples. The NMR partitioning method used in this study is based on the time-domain CIPHER inversion technique (Clerke, 2014) which employs a full spectral analysis of the combined pore system signal from NMR spectra (T2 distribution) and image porosity spectra, to partition the porosity using Gaussian decomposition instead of applying T2 cutoffs on T2 distribution (Figure 3). This combined spectrum has the spectral strength of both measurements, i.e., NMR for small to medium-sized pores and image data for the extra-large pores. The algorithm analyzes the combined pore body spectrum by fitting gaussian distributions at each depth level to locate and extract the specific volume, position, and width of the underlying gaussian modes (Macro, Micro1, and Micro23) which gives the best reconstruction of the input spectrum (Figure 4). The pore system classification used here is built upon separate maximum pore-throat diameter modal components (Ahr, 2005):

- Macro Porosity: pore diameter (Pd) > 4.62 microns
- Type 1 Micro Porosity: 0.35 < Pd < 4.62 microns
- Type 2/3 Micro Porosity: 0.09 < Pd < 0.35 microns

The quantification of these different pore systems in Reservoir M is used in the further petrophysical analysis for permeability, saturation, and rock typing.

Standard Archie cementation exponent values are applicable in carbonates with unimodal pore systems. In complex carbonates characterized by microporous grainstones and/or vugs, cementation exponent values differ from the typical values used. In this study, the pore partitioning outputs were used to calculate a variable continuous cementation exponent m curve based on the Ramakrishnan-Bruggeman effective medium model (Ramakrishnan, 2001), which is then used to improve Archie's saturation estimations in reservoir M. The model can be used to calculate the saturation in each individual pore system (Ramamoorthy, 2019).

The permeability estimation can also be improved using the pore partitioning outputs. The permeability in carbonates with intergranular porosity can be estimated based on porosity and average pore size. The standard SDR carbonate permeability method which utilized the NMR T2 logarithmic mean as an indicator for pore size works well for such types of carbonates. However, when significant macro porosity is present, the macro pores become connected and significantly increase the permeability. It was found that the SDR method underestimates the permeability across the macroporous zones. For such zones, the Macro permeability equation is used which used the volume of macro porosity as an input. In reservoir M, both methods were combined to calculate the final permeability, a macro porosity cut-off was used to switch between the two methods.

The porosity partitions were used to build a carbonate rock types model that reflects the textural variations in Reservoir M and can be used for further reservoir modeling and producibility analysis. The model is based on carbonate rock classification developed by (Marzouk, 1998) that corresponds to Dunham classes and makes use of the proportions of the three pore partitions (Figure 5). Under the assumption that T2 relaxation time can be used as an indicator for pore throat diameter, NMR data can be used to derive primary drainage capillary pressure curves. The mean T2 distribution of each rock type is transformed into its pseudo-capillary pressure and associated saturation height functions using an appropriate PC to T2 scaling factor. (Ouzzane, 2006) validated the concept using MICP data from a Jurassic carbonate reservoir in the Middle East.

RESULTS

Electrical borehole images and NMR measurements obtained from the wells used in this study clearly show the textural variation and multiple pore systems in carbonates across reservoir M. Figure 6 shows an example of pay interval dominated by grainstones which exhibits different degrees of heterogeneities in the form of vugs/molds as observed on the borehole image. Vuggy porosity represents almost a third of the total porosity system and it was found to be a controlling factor for productivity in the reservoir. Figure 7 shows an example of a non-reservoir interval dominated by layered mudstones/wackestones with homogeneous texture.

Figure 8 presents the results of the first part of the integrated carbonate workflow applied in this study. The heterogeneous nature of Reservoir M is represented in the porosity partitions throughout the interval which was significant in successfully planning the horizontal wells in the field as well as identifying which layers are more prone to early water breakthrough. Borehole images were found useful to accurately calculate vuggy porosity in the middle interval as NMR signals were masked by hydrocarbon effects.

Figure 9 presents the results of the second part of the workflow. The final permeability in Reservoir M was computed as a combination of SDR permeability (in zones dominated with micro/meso porosity) and Macro permeability (in zones dominated with macro permeability), this permeability was found to correctly model the flow behavior and identify the super-k layers that affect the history matching of the dynamic model. Textural variations were accounted for in estimating water saturation, and a continuous Bruggeman cementation exponent was used to calculate the saturation with the Archie equation, resulting in a 5-10 % difference in saturation compared with standard Archie parameters across the main pay intervals. Carbonate rock types were also derived and reflected the textural variations in Reservoir M and can be further utilized in 3D reservoir modeling workflows and deriving the capillary pressure and saturation height functions.

REFERENCES

Ahr, W. M. (2005). Confronting the Carbonate Conundrum. *Schlumberger Oilfield Review*, 18-29.

Clerke, E. (2014). Wireline Spectral Porosity Analysis of the Arab Limestone—From Rosetta Stone to Cipher. *SPWLA 55th Annual Logging Symposium.* Abu Dhabi, UAE.

Marzouk, I. (1998). New Classification of Carbonate Rocks for Reservoir Characterization. *Abu Dhabi International Petroleum Exhibition and Conference.* Abu Dhabi.

Noufal, A. (2018). New Borehole Image Log Based Technique for Pore System Characterization Predicts Productive Intervals in a Tight Carbonate Reservoir in Abu Dhabi. *ADIPEC.* Abu Dhabi, UAE.

Ouzzane, J. (2006). Application of NMR T2 Relaxation to Drainage Capillary Pressure in Vuggy Carbonate Reservoirs. *SPE Annual Technical Conference and Exhibition.* San Antonio, Texas, USA.

Ramakrishnan, T. S. (2001). A Model-Based Interpretation Methodology for Evaluating Carbonate Reservoirs. *SPE Annual Technical Conference and Exhibition.* New Orleans, Louisiana.

Ramamoorthy, R. (2019). Towards a Petrophysically Consistent Implementation of Archie's Equation for Heterogeneous Carbonate Rocks. *SPWLA 60th Annual Logging Symposium.* The Woodlands, Texas, USA.

Yamada, T. (2013). Revisiting Porosity Analysis From Electrical Borehole Images: Integration of Advanced Texture and Porosity Analysis. *SPWLA 54th Annual Logging Symposium.* New Orleans, Louisiana.

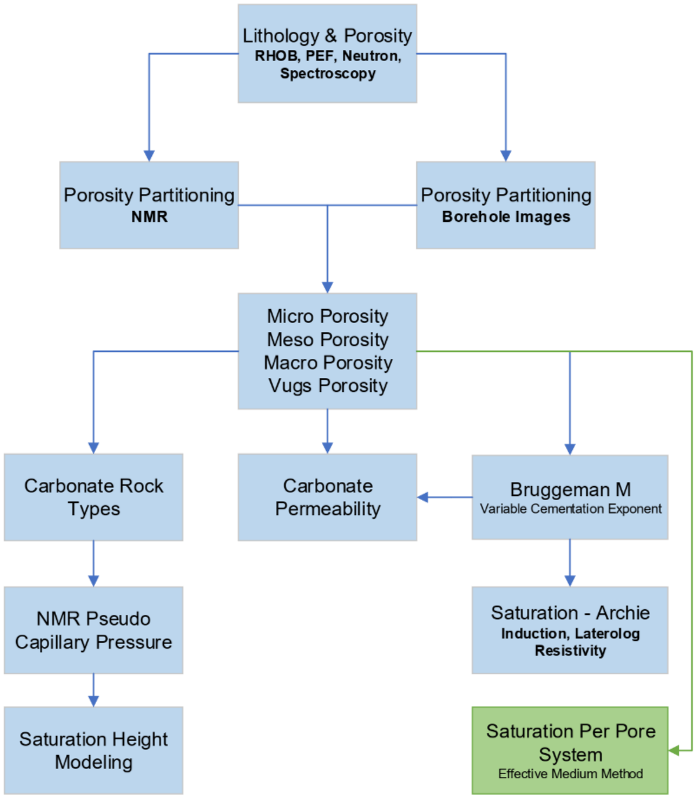

Figure 1: Carbonate Interpretation Workflow

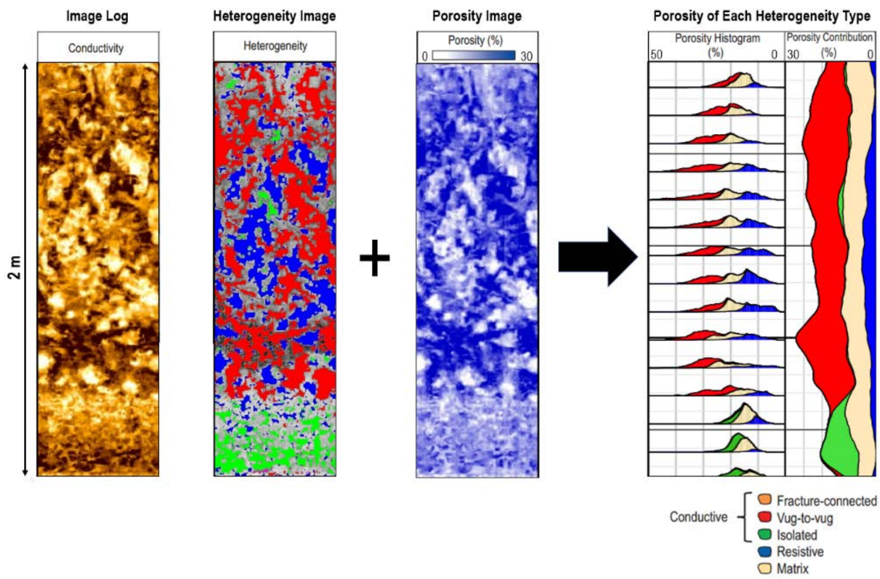

Figure 2: Image-based porosity partitioning in reservoir M. from left to right, dynamic image log (1st track), classified heterogeneity image (2nd track), porosity image (3rd track), porosity contribution per texture class using porosity image and the classified heterogeneity image (4th track).

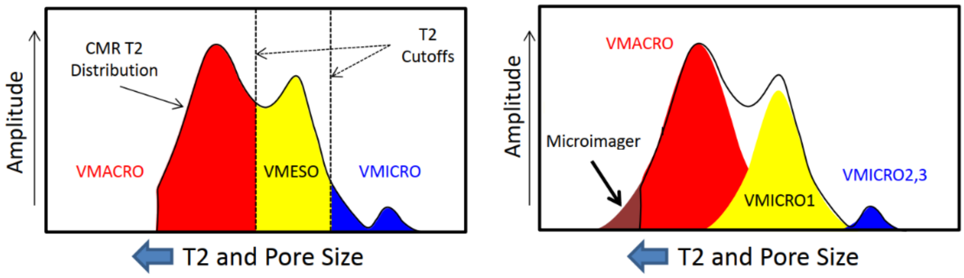

Figure 3: Traditional porosity partitioning using cutoffs in pore-body spectral data (left) vs CIPHER porosity partitioning fitting Gaussian distributions to reconstruct the NMR-Image composite pore-body spectrum (right). The "tail" corresponds to the larger pores extracted from image logs.

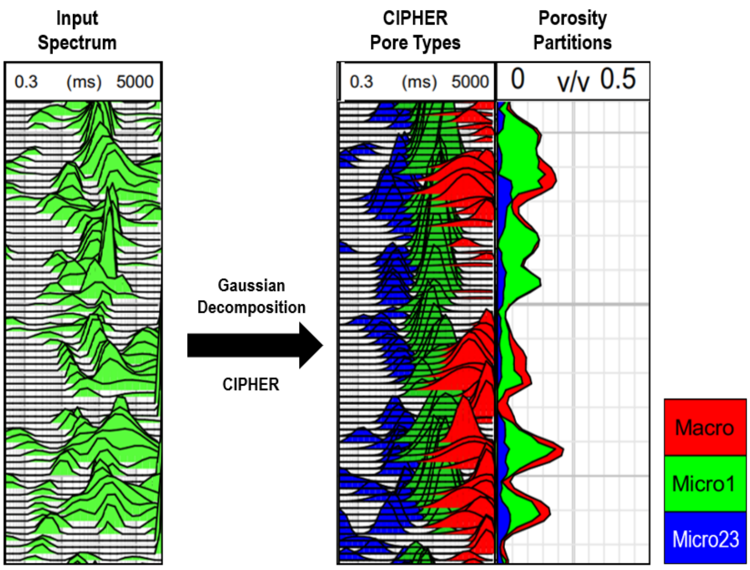

Figure 4: Spectral porosity analysis using CIPHER method in reservoir M to partition the combined porosity spectrum from NMR and image logs into 3 pore types (macro, micro1, micro23).

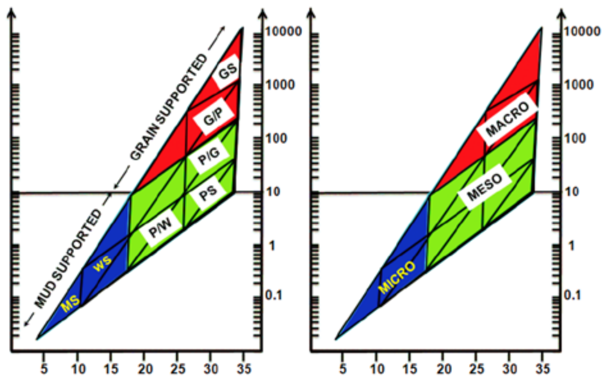

Figure 5: Carbonate rock classification based on porosity partitions and corresponds to Dunham classes. After Marzouk, 1998.

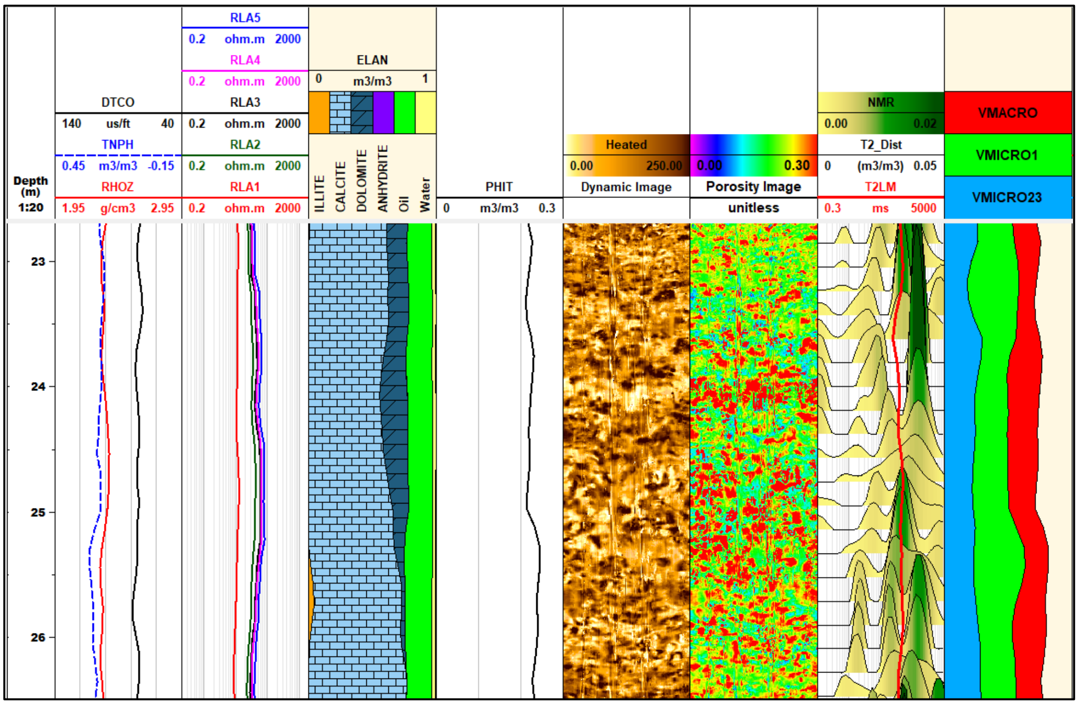

Figure 6: Example of grainstone facies in Reservoir M with abundant vuggy porosity.

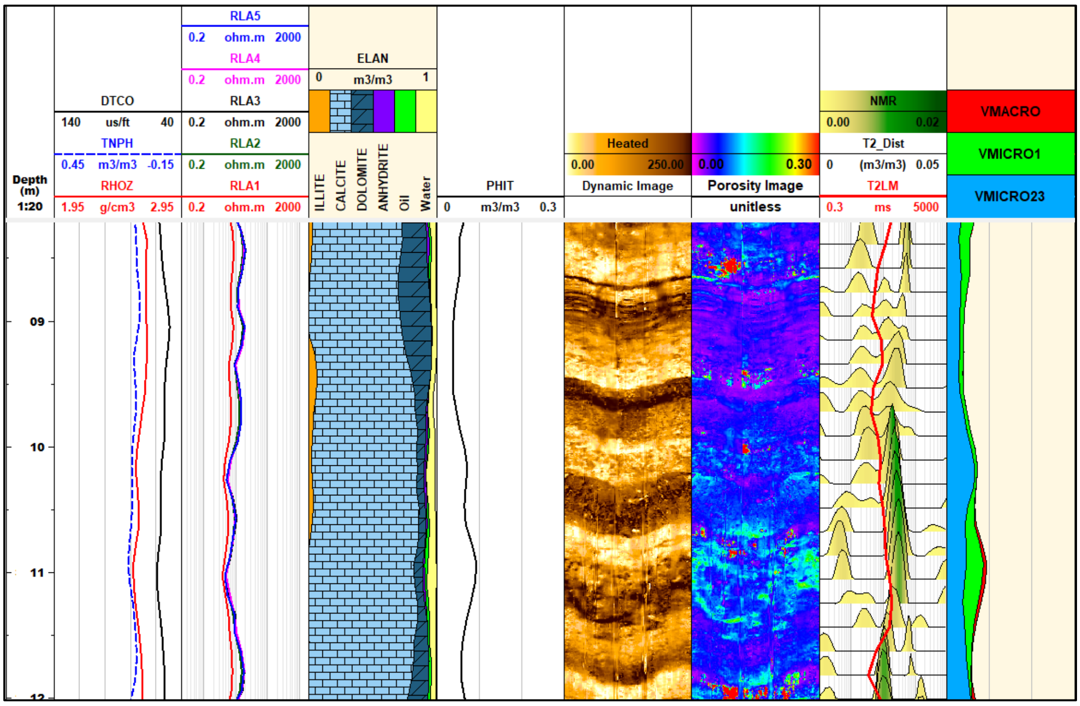

Figure 7: Example of mudstone/wackestone facies in Reservoir M.

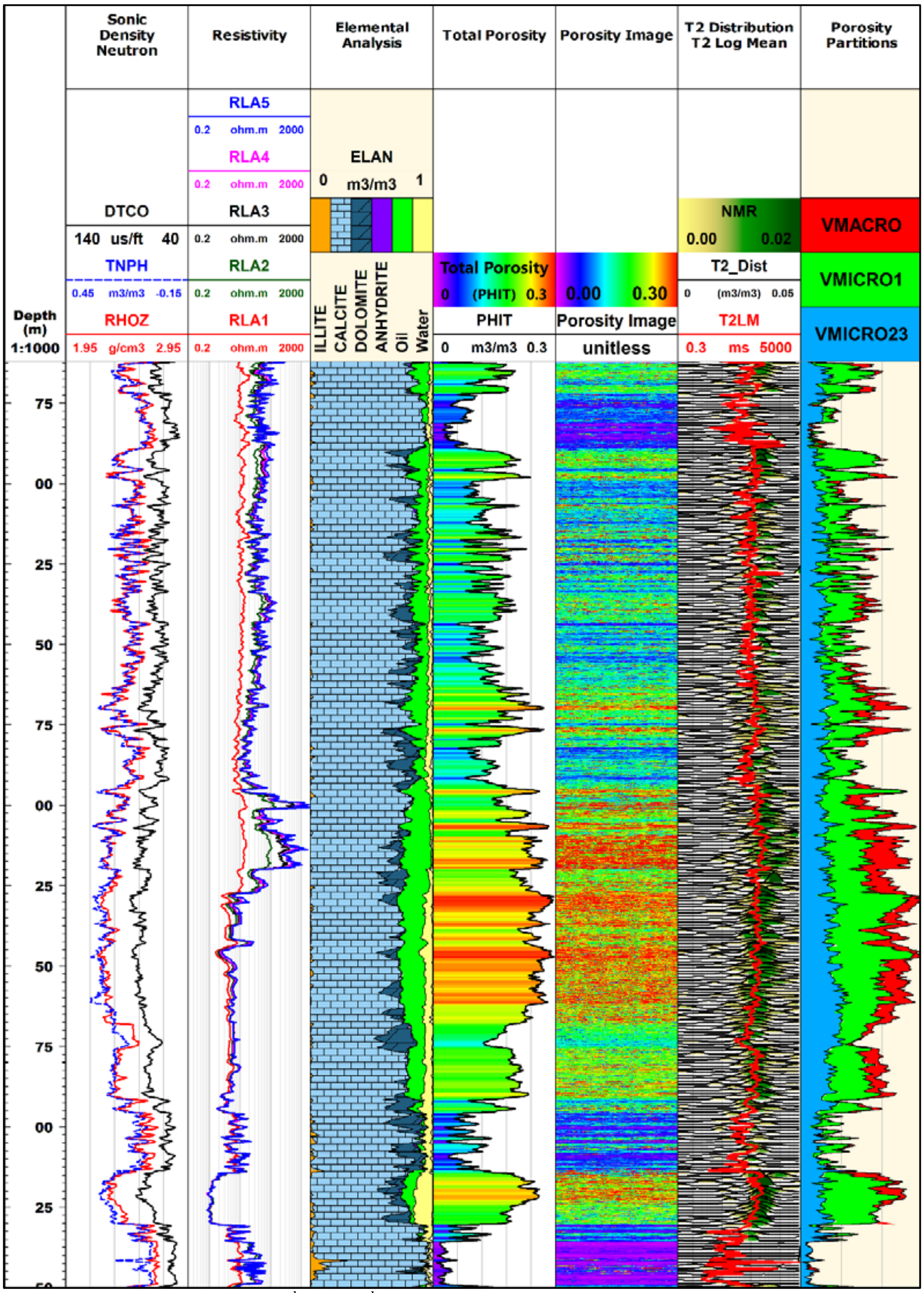

Figure 8: Standard openhole logs (2nd and 3rd track), Elemental analysis results (4th track), total porosity (5th track), porosity image generated from the resistivity borehole image (6th track), T2 distribution and logarithmic mean (7th track), final porosity partitioning (NMR & borehole image) using CIPHER technique (8th track) across reservoir M.

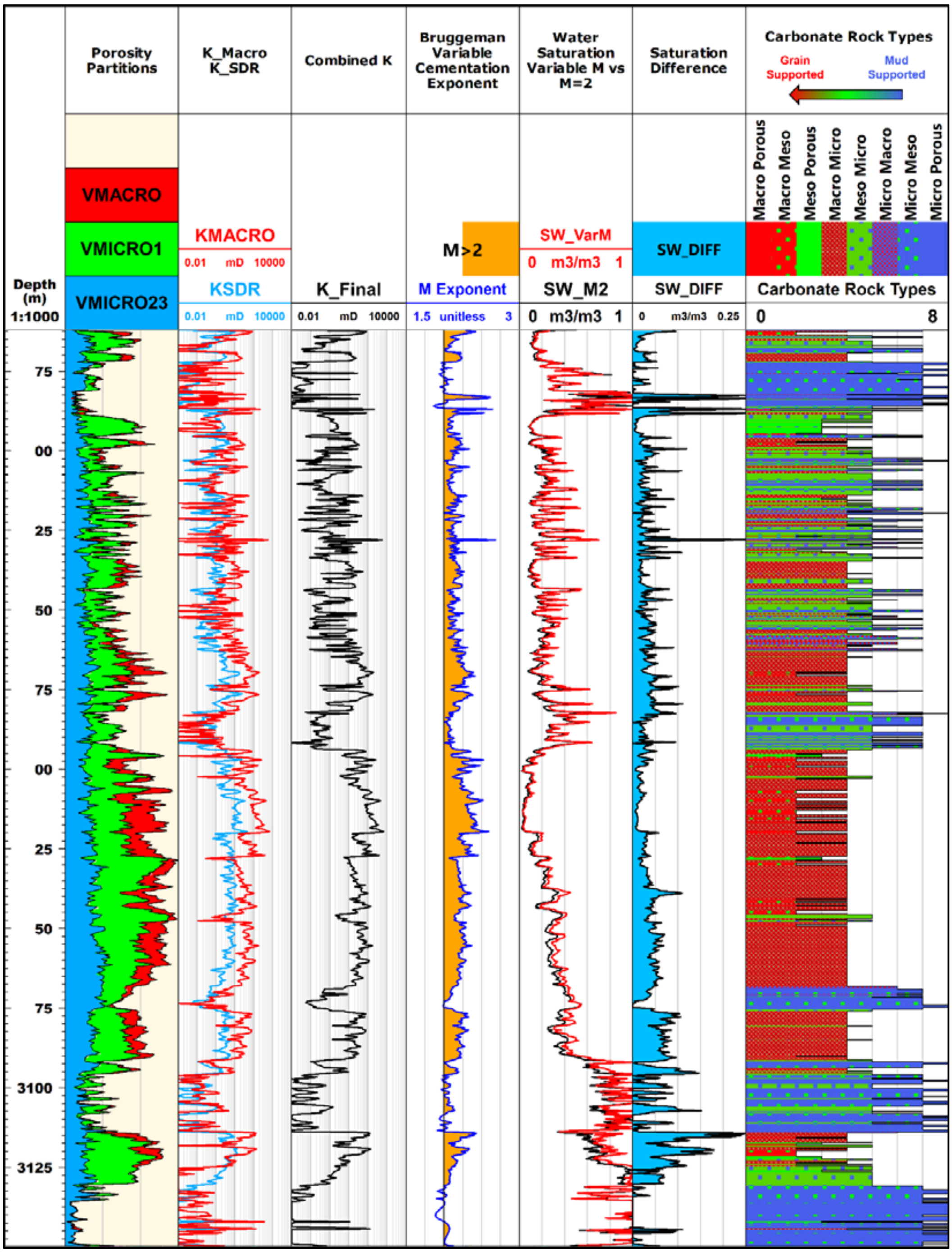

Figure 9: Results of integrated carbonate analysis in reservoir M. Porosity partitions (2nd track), SDR permeability and Macro permeability (3rd track), final combined permeability from KMACRO and KSDR (4th track), Cementation exponent M using Ramakrishnan-Bruggeman model (5th track), water saturations using Bruggeman cementation exponent and M=2 (6th track), water saturation difference between the two saturation curves (7th track), carbonate rock types (8th track).